ULTRAFAST SPECTROSCOPY OF THERMAL TRANSPORT AND ENERGY CONVERSION

Xu, X.*, Iyer, V., Wang, Y., Guo, L., and Yao, Q.
*Author for correspondence
Department of Mechanical Engineering and Birck Nanotechnology Center,
Purdue University,
West Lafayette IN,
USA
E-mail: xxu@ecn.purdue.edu

ABSTRACT

We use ultrafast spectroscopy to investigate a number of ultrafast thermal transport processes, and this paper is intended to provide a review of two applications of the method: one on direct probing of the atomic vibrations in thermoelectric materials; the other on the thermal transport across metal-dielectric interface. Atomic vibrational behaviors in thermoelectric materials are important for thermoelectric energy conversion. In misch-metal (Mm) filled (p-type) and single (La, Ba, or Yb) filled (n-type) antimony skutterudites, a high temperature thermoelectric materials for waste heat recovery, different filling species cause coupled vibrational modes between the guest atoms and the host lattice at different frequencies, which scatter phonons in different spectral spans and help to lower the lattice thermal conductivity and improve the thermoelectric figure of merit. The scattering processes of the different filling species are probed using ultrafast spectroscopy. Furthermore, using the Debye model for the measured lattice thermal conductivity together with the measured vibration frequencies and scattering rates, it is shown that the scattering due to the coupled vibrational modes has a considerable contribution to the suppression of lattice thermal conduction. Heat transfer processes at an interface between two materials are also of importance in many electronic devices. The electron-phonon coupling at a metal-dielectric interface is studied using the ultrafast spectroscopy, on the samples of gold thin films on silicon substrates. The two-temperature model is used to obtain the electron-phonon interface resistance or conductance at the gold-silicon interface, which quantifies the direct metal electron to dielectric phonon coupling strength. The effects of film thickness and probing wavelength are investigated in detail along with a Drude-Lorentz model to obtain a good estimate of interface thermal resistance/conductance. This work demonstrates the ultrafast spectroscopy as a powerful technique for thermal transport research.

INTRODUCTION

Caged compounds such as skutterudites and clathrates filled with guest atoms are found to have a significantly reduced thermal conductivity and high figure of merit (ZT), favorable for being used as thermoelectric materials [1, 2]. Binary skutterudites have the general chemical formula MX3, where M denotes a transition metal atom and X represents a pnictogen atom. The structure of a typical skutterudite is shown in Figure 1. The structure contains vacancies that can be filled with guest atoms, which significantly lower the thermal conductivity of the material through interaction with the phonons in the host lattice.

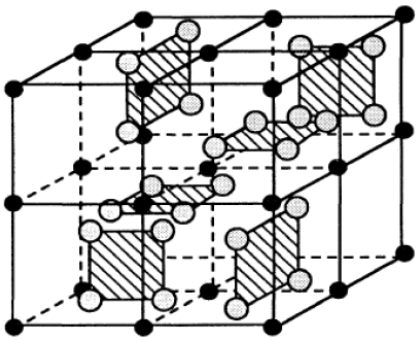

Figure 1. Structure of Skutterudite. Two of the eight cubes can be filled with guest atoms

Several theories have been proposed for the mechanism of lattice thermal conduction suppression [3-6]. We use ultrafast spectroscopy to investigate resonant interactions between guest atoms and the host lattice in filled-skutterudites, which act as additional scattering centers of acoustic phonons and therefore are the major mechanisms that reduce the lattice thermal conductivity.

For a material system consisting of metal and dielectrics, the interface heat transfer is one of the major concerns, for example, in the design of microscale and nanoscale electronic devices. In metal, electrons and phonons are both energy carriers while in dielectrics, phonons are the main energy carrier. Therefore, for metal-dielectric composite structures, heat can transfer across the interface by coupling between phonons in metal and dielectric or by coupling between electrons in metal and phonons in dielectric through electron interface scattering. Phonon–phonon coupling has been studied

mainly by the acoustic mismatch model and the diffuse mismatch model [7]. As for electron–phonon coupling, there are different viewpoints. Some studies have assumed that electron–phonon coupling across a metal-dielectric interface is negligible and heat transfer occurs as electron–phonon coupling within metal and then phonon–phonon coupling across the interface [8]. Electron–phonon coupling between metal (Cr, Ti, Al, Ni, and Pt) and SiO2 has exhibited negligible apparent thermal resistance using a parallel-strip technique [9]. On the other hand, our comparison between two-temperature model [10, 11] simulations and transient thermal reflectance (TTR) measurements for Au-dielectric interfaces reveals that energy could be lost to the substrate by electron-interface scattering during ultrafast-laser heating, and this effect depends on electron temperature and substrate thermal properties [12]. In this work, we use ultrafast spectroscopy to show the direct electron-phonon coupling at the metal-dielectric interface, and determine this coupling strength quantitatively. Our study also indicates the use of appropriate probe wavelengths [13] to obtain a better interpretation of the data, which has not been thoroughly investigated in the past studies on interface thermal transport involving gold. [14-16]

NOMENCLATURE

k	[W/mK]	Thermal conductivity
k_B	[m^2kg/Ks^2]	Boltzmann constant
v	[m/s]	Sound velocity
T	[K]	Temperature
$\hbar$	[m^2kg/s]	Reduced Planck's constant
θ_D	[K]	Debye temperature
τ	[s]	Phonon relaxation time
ω	[rad/s]	Frequency
C	[m]	Volumetric heat capacity
G	[W/m^3K]	Electron-phonon coupling factor
R	[-]	Reflection coefficient
δ	[m]	Optical penetration depth
δ_b	[m]	Electron ballistic length
t_p	[s]	Pulse duration
x	[m]	x coordinate
J	[W/m^2]	Pump fluence
ε	[-]	Dielectric constant
Γ_0	[1/s]	Drude damping term
L_i	[-]	Lorentz oscillator terms
h_0	[W/Km^2]	Room temp thermal conductance

Subscripts

L	Lattice
e	Electron in metal
p	Phonon in metal
s	Phonon in substrate

ULTRAFAST SPECTROSCOPY OF VIBRATIONAL DYNAMICS IN FILLED SKUTTERUDITES

For the filled-skutterudite samples, high-purity Co and Sb shots were pre-melted by induction at 1400^{0}C in boron nitride crucibles, followed by adding guest elements and Sb to reach the desired composition and re-melting at 1200^{0}C for 5 min. These ingots were then annealed at 750^{0}C for 2 weeks to obtain homogeneous samples. The annealed samples were ground into powder for spark plasma sintering. The resulting samples were dense and nearly single phase.

Ba, Yb, and La were chosen as the fillers since they have been found to have substantially different vibrational frequencies and are therefore capable of scattering a broad range of phonons. Mm was also used instead of pure rare-earth metals because of lower cost but similar performance. The skutterudite samples were fabricated by General Motors.

EXPERIMENTAL SETUP

The ultrafast pump-and-probe spectroscopy technique is used in a collinear scheme to measure the thermo-reflectance signal. The laser pulses are generated by a Spectra Physics Ti:Sapphire amplified femtosecond system with a central wavelength of 800 nm and a repetition rate of 5 kHz. The wavelength of the pump beam is then converted to 400 nm with a second harmonic crystal. The pump beam is mechanically chopped at 500 Hz to obtain better signal-to-noise ratio. The typical setup is shown in Fig. 2. For skutterudite samples, the probe beam is 800 nm. The setup is similar for studying interface transport of gold on silicon, except than an optical parametric amplifier (OPA) is used in some experiments to generate wavelengths near the interband transition threshold of gold (~500 nm). The probe beam is delayed in time with respect to the pump beam by using a computer controlled delay stage. Part of the probe beam is sent to one arm of a balanced photodetector and the other arm collects the reflected beam from the sample. The difference in signals is amplified with a preamplifier and read out using a lock-in amplifier referenced to the chopping frequency.

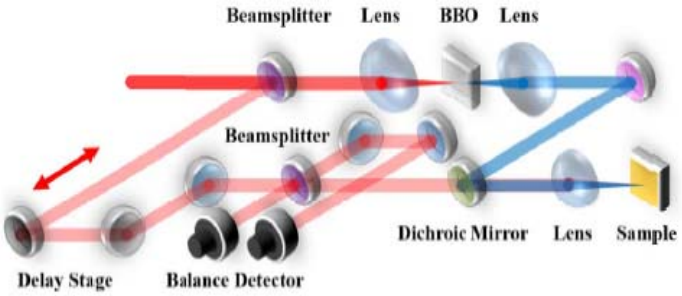

Figure 2 Transient thermo-reflectance setup

THEORETICAL MODEL

The model the thermal transport in skutterudites, the Debye model is used to fit the experimental thermal conductivity data.

$$k_L = \frac{k_B}{2\pi^2 v}\left(\frac{k_B T}{\hbar}\right)^3 \int_0^{\frac{\theta_D}{T}} \frac{x^4 e^x dx}{\tau^{-1}(e^x - 1)^2} \qquad (1)$$

The phonon relaxation time is given as:

$$\tau^{-1} = \frac{v}{L} + A\omega^4 + B\omega^2 T \exp(-\frac{\theta_D}{3T}) + \frac{1}{\tau_0}\exp[\frac{-(\omega-\omega_0)^2}{\omega_b^2}] \quad (2)$$

The four terms in Eq. (2) represent scattering by grain boundary, point defects, phonon-phonon Umklapp processes, and the coupled mode, respectively. Umklapp scattering results in a change of the total phonon momentum unlike normal scattering, which conserves momentum. This has an important effect on thermal conductivity because as phonon momentum decreases, the thermal conductivity also reduces. Coupled mode scattering is the main focus in our work. This occurs because of the coupling between host lattice and guest atoms that scatter phonons. τ_0 (decay time) and ω_0 (damping frequency) are obtained from our experiments by fitting the reflectance signal with a linear damped harmonic oscillator model. The variables L, A, B, and ω_b are fitted to the experimentally measured thermal conductivity. L is the grain boundary size and ω_b is the broadening term.

RESULTS

Transient reflectance signal for the n-type skutterudite sample is presented in figure 3 [17], after applying a filter to remove the carrier signal. Oscillations are caused by the vibrations of the filled species. A linear damped oscillator model is used to extract the oscillation frequencies and decay rate.

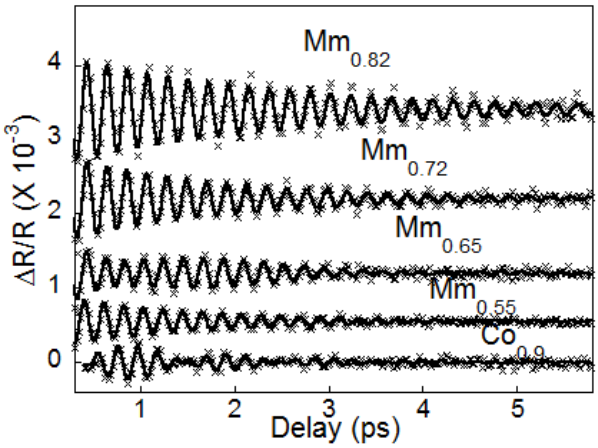

Figure 3. Oscillatory signals after the carrier signals are removed. The frequency is about 4.6 THz, close to, but distinct from the Raman frequency of Ag mode.

The fitting to experimental data using the Debye model is shown in figures 4 and 5 for misch metal filled p-type sample and Ba, Yb, La, and triple (Ba, Yb, and La) filled n-type samples.[17, 18] It is shown the Debye model can well describe the thermal conductivity over a wide temperature range.

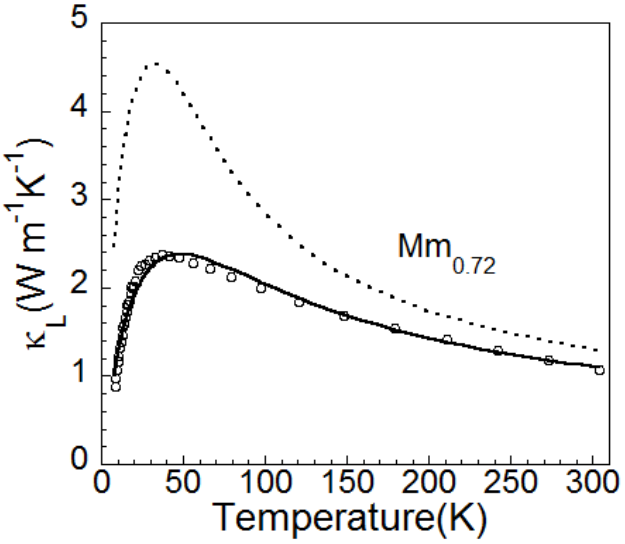

Figure 4. Dashed line shows thermal conductivity without resonant oscillation term and solid line fits the data with the oscillation term. Oscillation term contributes significantly to lowering of thermal conductivity.

DISCUSSION

As we have seen in the Debye model, the phonon scattering has several contributions. These are compared in figure 6 [18]. As evident, the resonance scattering term plays an important role. The other terms will be approximately of the same order for unfilled skutterudites. The appearance of the new resonance scattering due to filling leads to decreased lattice thermal conductivity

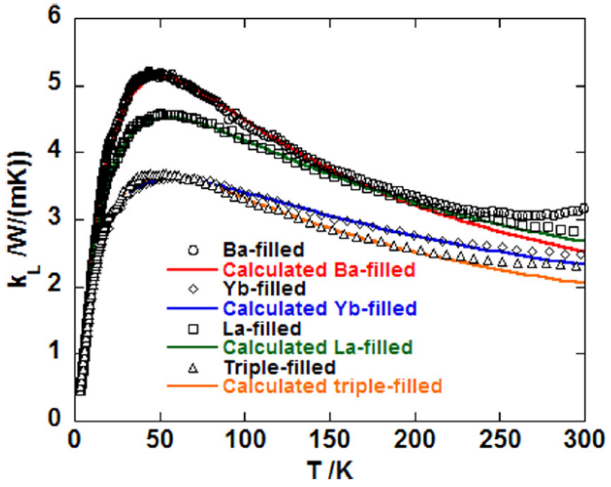

Figure 5. The experimental thermal conductivity is fit with the theoretical model for p-type samples.

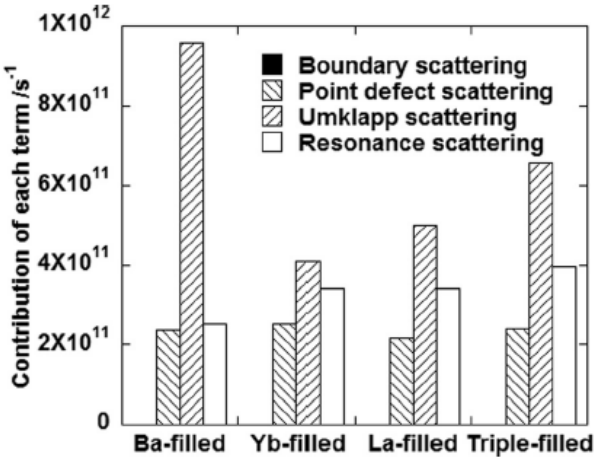

Figure 6. Contributions of different scattering mechanisms in reducing thermal conductivity for n-type samples.

Raman spectroscopy of the skutterudite samples was done to obtain the lattice resonance frequencies and compare them to the frequencies obtained from ultrafast measurements. From figure 7 [18], it can be seen that frequencies match very closely but are slightly different. The advantage of using the ultrafast measurement is that the relaxation time τ_0 can also be determined which is not possible in Raman experiments. The difference in the vibration frequencies is due to the fact that the ultrafast measurements probe the interactions between the filled species and the host lattice, while the Raman spectroscopy only measures the lattice behavior.

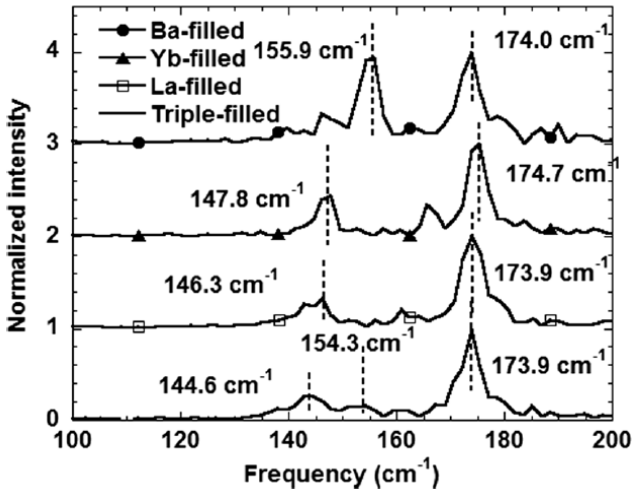

Figure 7. Raman spectra of the different n-type skutterudite samples showing a close match with frequencies obtained from ultrafast spectroscopy. The dashed lines indicate the ultrafast measurement frequencies.

ULTRAFAST HEAT TRANSFER ACROSS METAL DIELECTRIC INTERFACE

For investigating heat transfer across metal-dielectric interface, Au–Si samples of varying Au thicknesses were prepared by thermal evaporation at a pressure of the order of 10^{-7} Torr on to silicon substrates. The thicknesses of the gold films are 39, 46, 60, 77, and 250 nm, measured using an atomic force microscope.

THEORETICAL MODEL

Interface heat transfer was modelled using a two temperature model (TTM):

$$C_e \frac{\partial T_e}{\partial t} = k_e \frac{\partial^2 T_e}{\partial x^2} - G(T_e - T_p) + S \tag{3}$$

$$C_p \frac{\partial T_p}{\partial t} = k_p \frac{\partial^2 T_p}{\partial x^2} + G(T_e - T_p) \tag{4}$$

The boundary conditions are:

$$T_e(t=o) = T_p(t=o) = T_s(t=o) = T_0 \tag{5}$$

$$-k_e \left.\frac{\partial T_e}{\partial x}\right|_{x=L} = \left.\frac{T_e - T_s}{R_{es}}\right|_{x=L} \tag{6}$$

$$-k_p \left.\frac{\partial T_p}{\partial x}\right|_{x=L} = \left.\frac{T_p - T_s}{R_{ps}}\right|_{x=L} \tag{7}$$

$$-k_s \left.\frac{\partial T_s}{\partial x}\right|_{x=L} = \left.\frac{T_e - T_s}{R_{es}}\right|_{x=L} + \left.\frac{T_p - T_s}{R_{ps}}\right|_{x=L} \tag{8}$$

Here R_{es} is the interface electron-phonon resistance. R_{ps} is the interface phonon-phonon resistance. The laser source S is expressed as:

$$S = \frac{0.94(1-R)J}{t_p(\delta+\delta_b)[1-\exp(-\frac{L}{\delta+\delta_b})]} \exp[-\frac{x}{\delta+\delta_b} - 2.77(\frac{t}{t_p})^2] \tag{9}$$

We can then relate the temperature to the dielectric constant using the Drude (-Lorentz) model and then obtain the reflectance R of the probe laser beam. Thus we can fit the TTR measurements with this approach and obtain R_{es} and R_{ps} as fitting parameters. The G value can be obtained from bulk gold sample and neglecting the interface effects.

The commonly used Drude-Lorentz model for gold is: [19]

$$\varepsilon = \varepsilon_\infty - \frac{\omega_p^2}{\omega(\omega + i\Gamma_0)} + L_1(\omega) + L_2(\omega) \quad (10)$$

Where ω_p stands for plasma frequency

$$L_i(\omega) = D_i\left[e^{i\phi_i}(\omega_i - \omega - i\Gamma_i)^{\mu_i} + e^{-i\phi_i}(\omega_i + \omega + i\Gamma_i)^{\mu_i}\right] \quad (11)$$

$$\Gamma_i = A_{eei}T_e^2 + B_{epi}T_p + Y_i \quad (12)$$

The coefficient describing electron-electron scattering A_{ee0} is taken as 1.2×10^7 $s^{-1}K^{-2}$ which is obtained from the low temperature Fermi liquid theory [20]. B_{ep0} is chosen as 3.6×10^{11} $s^{-1}K^{-1}$ which is predicted by matching the experimental results of dielectric constant at room temperature [21]. We also found that a temperature-independent term Y_i needs to be included in the expression for the Lorentzian oscillators, in order to fit the temperature-dependent dielectric function (Y_0 is taken to be 0). The electron-electron scattering rate of Lorentzian oscillators A_{ee1}, A_{ee2} are assumed to be the same as that in the Drude model A_{ee0}. B_{ep1}, B_{ep2} are determined using room temperature optical constants with Eq. 12. Y_1 , Y_2 are found to be 7.9×10^{14} rad/s and 1.9×10^{15} rad/s respectively.

The Reflectance is calculated with the standard Fresnel equation: [22]

$$R = \frac{|\varepsilon| - \sqrt{2(\varepsilon_1 + |\varepsilon|)} + 1}{|\varepsilon| + \sqrt{2(\varepsilon_1 + |\varepsilon|)} + 1} \quad (13)$$

$$|\varepsilon|^2 = \varepsilon_1^2 + \varepsilon_2^2 \quad (14)$$

Where ε_1 and ε_2 are the real and imaginary parts of the dielectric constant respectively. In a series of papers [12, 23, 24] we presented details of these models including estimation of the coupling factor G.

RESULTS

Figure 8 [12] presents the initial interface heat transfer study with 400nm pump and 800 nm probe. Figure 9 [23] shows the probe study and 490nm probe with Drude-Lorentz model is presented in figure 10 [24].

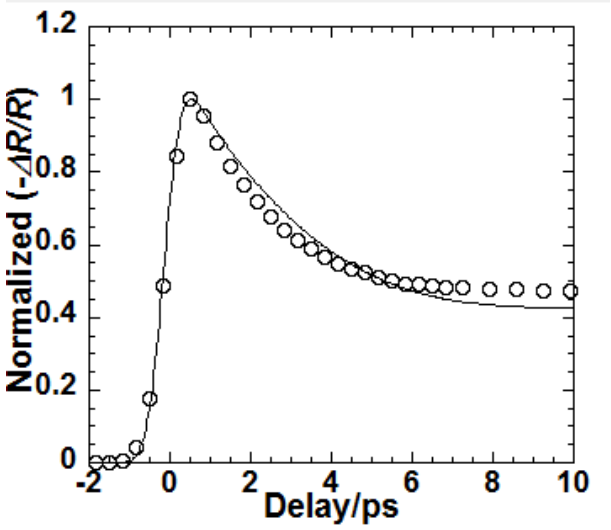

Figure 8. TTM used to fit the TTR measurement for 60 nm thin film gold on Si. The probe is 800 nm and Drude model is used.

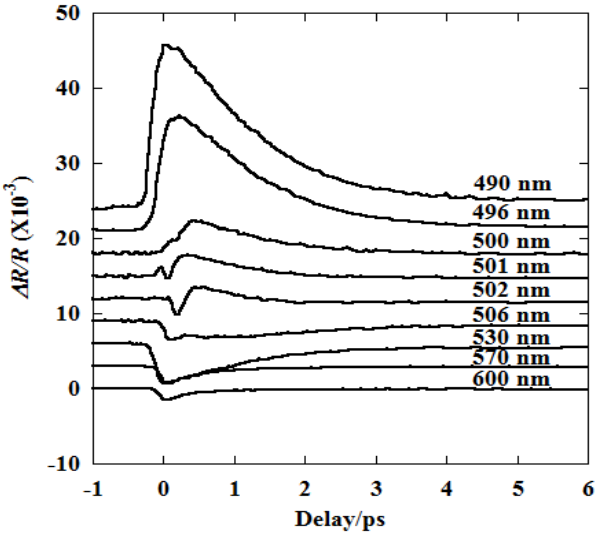

Figure 9. We obtain the highest reflectance change near 490nm probe which is chosen for the next study. Plots are vertically shifted for clarity

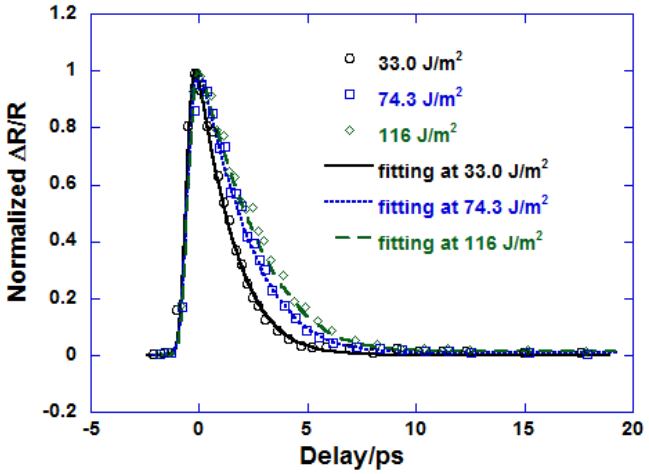

Figure 10. Fitting for 65 nm gold film, using 490 nm probe and Drude Lorentz model

It should be noted that all results presented in this paper are only representative of a larger set. More details can be found from [12, 23, 24].

DISCUSSION

Following photoexcitation, electrons relax back to the fermi-level by losing their energy to phonons. At an early stage a non-thermalized distribution, which does not follow the Fermi-Dirac distribution is in place. After about 100 fs, the electrons form a Fermi-Dirac thermalized distribution which can be well described by an electron temperature. Therefore we stretched the laser pulses to avoid non-thermalized electrons (figure 11 [12]). It is incorrect to use TTM with non-thermalized electrons.

Figure 12 shows a schematic of electron distribution change near the fermi-level [24]. The change in occupation (Δf) is maximum closest to the fermi level, therefore leading to a large change in probe reflectivity. The 490 nm probe is slightly above fermi-level (d to s band transition) so as to capture the peak in the Δf caused due to pump excitation. Thus from our study using 800 nm probe, we showed the significance of selecting the correct probe and carrier out the next study with a 490 nm probe.[23]

After obtaining the interface thermal resistance using fitting, we proceed to write the inverse of the interface resistance, the interface conductance in the form:

$$h(T) = h_0(C(T_e + T_l) + 1) \qquad (15)$$

h_0 represents the conductance when the electron and phonon temperatures are low. h_0 and C are found from the data in Fig. 13 [24] as 1.1×10^8 W/(Km^2), and 1.8×10^{-3} K^{-1}. Thus the room temperature value of interface conductance is obtained as 1.1×10^8 W/(Km^2). Furthermore the room temperature electron-phonon coupling factor in bulk gold, G_0 is found to be 1.4×10^{16} W/(m^{3}K).

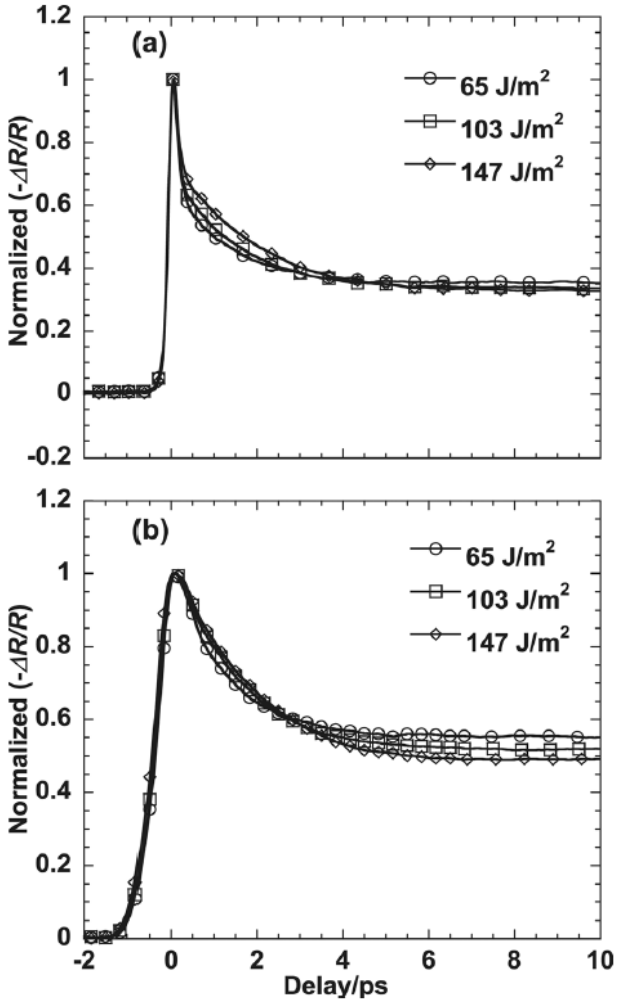

Figure 11. Pulse duration increased to avoid effect of non-thermalized electrons. (a) shows 100fs pump (b) is 380 fs.

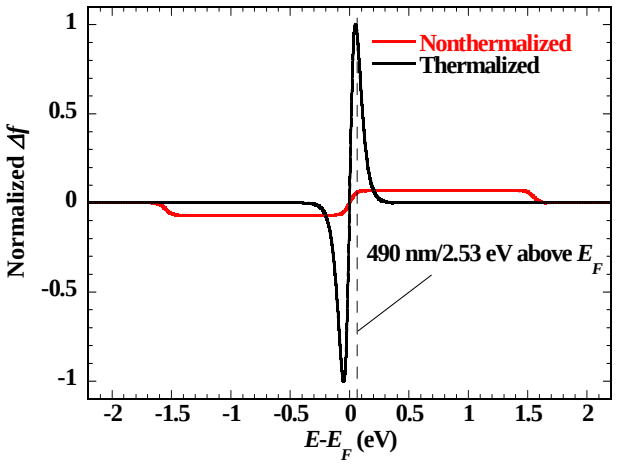

Figure 12. Probing near the Fermi-level, where thermalized electrons relax to, produces maximum signal

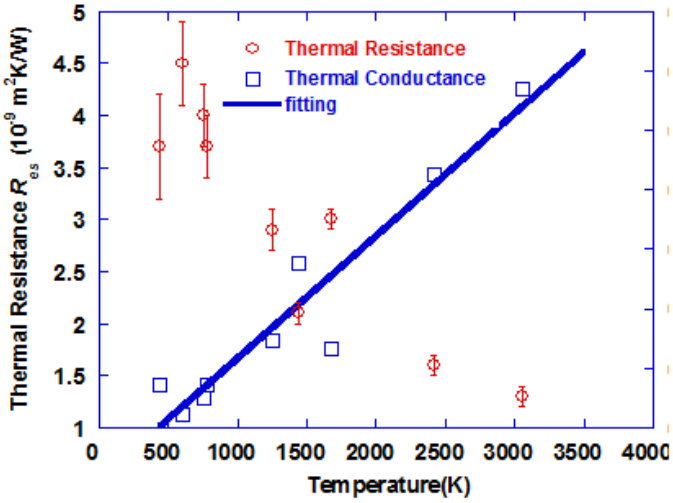

Figure 13. Room temperature thermal resistance obtained by extrapolation.

CONCLUSIONS

In conclusion, we have studied the ultrafast dynamics in technologically important skutterudite thermoelectric materials to understand the fundamental reasons for decrease in lattice thermal conductivity. Our study shows that resonant coupling between lattice and guest atoms leads to better phonon scattering, ultimately decreasing thermal conductivity. Interface heat transfer studies for gold on silicon substrate were also carried out. Further clarifications on the electron occupation and corresponding probing energies were made leading to an improved and reliable experimental technique. The popularly used Drude model was also improved with a Drude-Lorentz model to develop a better theoretical framework. Electron-phonon thermal resistance/conductance at a gold-silicon interface was quantified.

ACKNOWLEDGEMENT

Support to this work by the National Science Foundation and the Department of Energy (Award No. DE-EE0005432) is acknowledged.

REFERENCES

[1] Meisner, G., Morelli, D., Hu, S., Yang, J., and Uher, C., 1998, Structure and lattice thermal conductivity of fractionally filled skutterudites: Solid solutions of fully filled and unfilled end members, *Physical Review Letters*, 80(16), pp. 3551-3554.

[2] Nolas, G., Takizawa, H., Endo, T., Sellinschegg, H., and Johnson, D., 2000, Thermoelectric properties of Sn-filled skutterudites, *Applied Physics Letters*, 77(1), pp. 52-54.

[3] Bernstein, N., Feldman, J., and Singh, D., 2010, Calculations of dynamical properties of skutterudites: Thermal conductivity, thermal expansivity, and atomic mean-square displacement, *Physical Review B*, 81(13), p. 134301.

[4] Li, L., Liu, H., Wang, J., Hu, X., Zhao, S., Jiang, H., Huang, Q., Wang, H., and Li, Z., 2001, Raman spectroscopy investigation of partially filled skutterudite, *Chemical Physics Letters*, 347(4-6), pp. 373-377.

[5] Keppens, V., Mandrus, D., Sales, B., Chakoumakos, B., Dai, P., Coldea, R., Maple, M., Gajewski, D., Freeman, E., and Bennington, S., 1998, Localized vibrational modes in metallic solids, *Nature*, 395(6705), pp. 876-878

[6] Hermann, R., Jin, R., Schweika, W., Grandjean, F., Mandrus, D., Sales, B., and Long, G., 2003, Einstein oscillators in thallium filled antimony skutterudites, *Physical Review Letters*, 90(13).

[7] Cahill, D., Ford, W., Goodson, K., Mahan, G., Majumdar, A., Maris, H., Merlin, R., and Sr, P., 2003, Nanoscale thermal transport, *Journal of Applied Physics*, 93(2), pp. 793-818.

[8] Majumdar, A., and Reddy, P., 2004, Role of electron-phonon coupling in thermal conductance of metal-nonmetal interfaces, *Applied Physics Letters*, 84(23), pp. 4768-4770.

[9] Chien, H., Yao, D., and Hsu, C., 2008, Measurement and evaluation of the interfacial thermal resistance between a metal and a dielectric, *Applied Physics Letters*, 93(23), p. 231910.

[10] Kaganov, M., Lifshitz, I., And Tanatarov, L., 1957, Relaxation between electrons and the crystalline lattice, *Soviet Physics* Jetp-Ussr, 4(2), Pp. 173-178.

[11] Qiu, T., And Tien, C., 1993, Heat-transfer mechanisms during short- pulse laser-heating of metals, *Journal of Heat Transfer-Transactions of the Asme,* 115(4), pp. 835-841.

[12] Guo, L., Hodson, S., Fisher, T., and Xu, X., 2012, Heat transfer across metal-dielectric interfaces during ultrafast-laser heating, *Journal of Heat Transfer*-Transactions of the Asme, 134(4), p. 042402.

[13] Sun, C., Vallee, F., Acioli, L., Ippen, E., And Fujimoto, J., 1994, Femtosecond-tunable measurement of electron thermalization in gold, *Physical Review B*, 50(20), pp. 15337-15348.

[14] Brorson, S., Kazeroonian, A., Moodera, J., Face, D., Cheng, T., Ippen, E., Dresselhaus, M., And Dresselhaus, G., 1990, Femtosecond room-temperature measurement of the electron-phonon coupling constant-λ in metallic superconductors, *Physical Review Letters*, 64(18), pp. 2172-2175.

[15] Elsayedali, H., Juhasz, T., Smith, G., And Bron, W., 1991, Femtosecond thermoreflectivity and thermotransmissivity of polycrystalline and single-crystalline gold-films, *Physical Review B*, 43(5), pp. 4488-4491.

[16] Choi, G., Wilson, R., and Cahill, D., 2014, Indirect heating of Pt by short-pulse laser irradiation of Au in a nanoscale Pt/Au bilayer, *Physical Review B*, 89(6).

[17] Wang, Y., Xu, X., and Yang, J., 2009, Resonant oscillation of misch-metal atoms in filled skutterudites, *Physical Review Letters*, 102(17), p. 175508.

[18] Guo, L., Xu, X., Salvador, J., and Meisner, G., 2013, Coupled vibrational modes in multiple-filled skutterudites and the effects on lattice thermal conductivity reduction, *Applied Physics Letters*, 102(11), p. 111905.

[19] Etchegoin, P., Le Ru, E., and Meyer, M., 2006, An analytic model for the optical properties of gold, *Journal of Chemical Physics*, 125(16), p. 164705.

[20] Macdonald, A., 1980, Electron-phonon enhancement of electron-electron scattering in Al, *Physical Review Letters*, 44(7), pp. 489-493.

[21] Johnson, P. B., and Christy, R. W., 1972, Optical Constants of the Noble Metals, *Physical Review B*, 6(12), pp. 4370-4379.

[22] Pedrotti F. L., Pedrotti L. S., and Pedrotti L. M., 2008, Introduction to Optics, Pearson Education.

[23] Guo, L., and Xu, X., 2014, Ultrafast Spectroscopy of Electron-Phonon Coupling in Gold, *Journal of Heat Transfer*-Transactions of the Asme, 136(12), p. 122401.

[24] Yao, Q., Guo, L., and Xu, X., 2016, Ultrafast electron-phonon coupling at metal dielectric interface, *submitted.*